Aerosol Detection
(AI: Aerosol Index)
Algorithm Theoretical Basis Document
(AI-v1.0)

NMSC/SCI/ATBD/AI, Issue 1, rev.0
2015. .

Table of Contents

List of Tables

List of Figures

List of Acronyms

BT	Brightness Temperature
BTD	Brightness Temperature Difference
BTV	Background Threshold Value

1. Overview

Asian dust originates from Mongolian plateau and Gobi desert, dry area with less than 200mm of annual precipitation which is known as yellow earth plateau in Northern China. It is a phenomenon in which large amount of dust and sand float in air when strong wind blows in cold area at the back of cold front and fly far away along with the westerlies. Korea Environment Institute stated in its presentation in 2005 that at most 1,817,000 people are treated in hospitals, 165 people die in a year, plant growth is interrupted, and state of the high-tech industry is greatly impacted in Korea due to Asian dust. When tangible and intangible loss is converted into monetary value, it counts up to 7 trillion 3 hundred won (Lim et al. 1989). In a survey about type of Asian dust damage from (year) 2000 to 2004 done to 1,000 people nationwide, it was found that 35.4% have experienced disease due to Asian dust averaged 2 times a year. It is known that Asian dust contains silicon, iron, aluminum, lead and cadmium and increases the air concentration of heavy metal.

Observation of dust is essentially required in order to prevent and cope with the damage from Asian dust. Asian dust is detected on the ground and from satellites. Observation on the ground is accurate, and provides continuous observation, as well as detailed information on physical and chemical characteristics. However, a satellite observation with high temporal and spatial resolution is required to figure out the distribution and movement.

2. Background and Purpose

Aerosol monitoring using satellite uses radiation at different wavelength bands. Ultraviolet ray is suitable for aerosol detection since it has relatively less ground surface reflectance and less directional reflection effect by satellite and solar altitude (Torres et al., 2002). However, the signal of ultraviolet radiation is excessively low compared to visible and ultrared radiation.

The wavelength that is most widely used is visible light. However, visible light has very low sensitivity over desert due to relatively higher ground surface reflectance compared to ultraviolet radiation. Therefore, aerosol observation using this wavelength band is done only over ocean and vegetated area with low ground surface reflectance (Fukushima and Toratani, 1997; Kaufman et al., 1997; King et al., 1999;

Mishchenko et al. 1999; Stow et al., 1993; Torres et al., 2002).

Aerosol detection using infrared wavelength band is not suitable for aerosol measurement because the wavelength is larger than the aerosol particle. But, in the case of Asian dust, as its particle is larger than typical aerosol, the measurement using infrared is relatively effective than other aerosol detection methods (Ackerman et al, 1994). It also has advantage to be able to detect aerosol over high reflecting surface and at night.

An aerosol detection method with infrared uses brightness temperature Difference(BTD) of 3.7㎛ and 11㎛, which apply to window area in the atmosphere (Ackerman, 1989). However, as 3.7 ㎛ channel is greatly affected by altitude of sun, satellite and earth surface, large error could occurs in aerosol detection using this channel. Another method uses the difference between 11 ㎛ and 12 ㎛ BTD suggested by Prata(1989). Wen and Rose(1994)and Gu et al. (2003) calculated the particle size, optical thickness, and total mass of volcanic ash aerosol, by applying that the BTD difference between 11 ㎛ and 12 ㎛, which is shown as negative in the case of aerosol loading in the air, whereas it shows positive in the case of water accumulation like cloud with Advanced Very High Resolution Radiometer (AVHRR). Gu et al.(2003) applied this method to Moderate Resolution Imaging Spectrometer (MODIS) to measure the Asian dust in the eastern Asian region. However, they reported that the calculated quantity of aerosol could have very large error by 10~40% depending on refractivity, size distribution, particle shape of the particle used as input data in the air radiation model. Currently, Korean Meteorological Administration is applying BTD method to AVHRR data, using –0.7°K for the threshold value to distinguish Asian dust and cloud. However, this threshold value could be affected by optical characteristics of aerosol and the condition of earth surface and air. Therefore, accurate adjustment is required because the threshold value can vary with location and time.

3. Algorithm

3.1. Theoretical Background

Because there always exists water vapor in the atmosphere, the BTD will be slightly a positive value. This meams that the BTD threshold value can vary depending on

atmospheric condition. In a clear air condition without aerosol, variation the BTD threshold value has been analyzed with respect to zenith angle of satellite and sun, perpendicular distribution of temperature and humidity in the air, earth surface temperature and emissivity, and earth surface reflectance. In addition, in the presence of aerosol loading, the BTD sensitivity has been analyzed with respect to atmospheric composition, profile in a given standard air condition. The selected period is~~was~~ the Asian dust season in March and April when Asian dust affects Northeastern Asia. Atmosphere radiation model used in sensitivity analysis was Rstar5b developed by CCSR(Center for Climate System Research).

3.1.1. Model Input Material

In Rstar5b, various input data can be used depending on a given solar zenith angle (Θ_0), zenith angle of satellite(Θ), surface reflectance(α_s), optical thickness of aerosol at 0.5 μm($\tau_{0.5\mu m}$), earth surface temperature and emissivity, vertical distribution of temperature and humidity, aerosol and cloud, Seven satellite and zenith angles between 10 and 80 degree, and Eight aerosol optical thickness with 0.4 interval between 0 and 2.8 have been used.

In order to obtain accurate sensitivity analysis through radiative transfer model, the response function of the sensor is required. In this study, we have used MODIS response function.

3.1.2. Optical Model of Aerosol

For an accurate sensitivity study, an optical model that can describe the size distribution of aerosol should be selected and also optical properties according to the composition of aerosol should be understood. There were previous studies about the ways of determination of aereosol size distribution. Power law size distribution was used to determine the aerosol size distribution in stratosphere or troposphere (Toon and Pollack, 1976) and multiple mode size distribution can be used considering that aerosol is formed through different physical processes (Whitby, 1978). As seen above, since particle size distribution can have one or more mode, we used the equation (1) assuming average radius 0.25∽2.0 μm enabling long distance transportation and bi-modal log normal size distribution. This equation has two modes which have each

maximum value in both sides of 0.6 ㎛, respectively.

$$\frac{dV}{dlnr} = \sum_{n=1}^{2} \frac{C_{v,i}}{\sqrt{2\pi} S_i} \exp[-\frac{1}{2}(\frac{\ln r - \ln r_{v,i}}{S_i})^2] \quad (1)$$

Here, subscript i refers to each mode number of bi-modes. $C_{v,i}$ refers to volume concentration in bi-modes, $r_{v,i}$ refers to average radius of aerosol, and S_i refers to standard deviation of $\ln r$. For variables included in size distribution in bi-modal log normal, AERONET(AErosol RObotic NETwork) data in Anmyeondo area in March 20, 2001, when a lot of Asian dust cases were reported, was used. Model input variables used here were $C_{v,1}$=0.212768, $C_{v,2}$=0.591440, $r_{v,1}$=0.096918㎛, $r_{v,2}$ = 2.379725㎛, S_1=0.528396, and S_2=0.629815.

Optical properties of floating aerosol largely depend also on reflectance index, not only on particle size distribution (Sokolik and Toon, 1998). As optical property data of aerosol built in Rstar5b used in this study contains aerosol information not suitable for this sensitivity analysis, so instead of it, we used aerosol data of HITRAN(HIgh-resolution TRANsmission), one of the atmospheric radiation models. Analysis was done focusing on Asian dust particle. Diameter of Asian dust particle found in Chinese desert had maximum value in the range of 1~5 ㎛ , with mean diameter of 2 ㎛(Chun et al., 2001). It mainly consists of some chemical substances including SiO_2, Si, Fe, Al, and Ca, SiO_2 accounting for 60%(Goudie, 1978; McKendry et al., 2001). However, when the particle was large, its mineral composition was almost 100% pure quartz (SiO_2)particle. Therefore, reflectance index of quartz was used as input data of radiation model instead of Asian dust particle(Gomes and Gillette, 1993).

3.1.3. Result

1) Changes depending on types of aerosol

There are various kinds of aerosol in the atmosphere such as sand particle, volcanic ash and sea salt particle. To analyse the characteristics of them, BTD sensitivity change depending on aerosol composition and BT (Brightness Temperature) value at 11 ㎛ was applied. Atmospheric model variable based on Lowtran-7 was used

and US standard variable was adopted for temperature, humidity and chemical composition distribution in atmosphere. Zenith angle of sun and satellite was fixed to 40°. This zenith angle is the typical angle when Terra satellite observes over the Korean Peninsula, so the value was selected for accurate sensitivity analysis. As volcanic aerosol is emitted from high heat source and reaches to high altitude due to its generation mechanism, it was assumed to be layered at 10~15 km , and sea salt particle was assumed to be layered at 0~2 km. Other aerosol particle was assumed to be layered in 3~5 km (Yu and Rose, 2002; Shaw, 1980).

When the optical thickness of aerosol was 0, that is, in clear air condition, BTD showed threshold value of 0.8K. Prata(1989) regarded that it is volcanic aerosol when the BTD value is lower than 0K and it is cloud when the BTD is higher than 0K. However, the result from radiation model showed a threshold value higher than 0K. Therefore, we can infer that aerosol detection methodology based on threshold value of 0K has limitation. And we analyse the tendency of BTD change according to the increase of optical thickness. Sea salt particle showed positive value as optical thickness increases, but other aerosol showed negative value. When optical thickness increased from 0 to 1, quartz particle changes the most from 0.8K to -1.9K, followed by BTD change of volcanic ash aerosol. BTD at 11 ㎛ showed the biggest change in dust particle while sea salt particle showed the smallest BTD. Therefore, accurate aerosol information is necessary because the BTD change is different according to the aerosol composition.

2) Changes according to the location of sun and satellite

Radiation observed in a satellite is affected by satellite zenith angle, solar zenith angle, and azimuth difference of satellite and sun. Change of BTD and BT by the change of zenith angle was analyzed. Satellite zenith angle and azimuth difference between satellite and sun were fixed to 40° and 0°, respectively, and BTD according to the optical thickness and BT change at 11 ㎛ were estimated when solar zenith angle was 10, 30, 50, and 80°. Threshold value of BTD and BT at 11 ㎛ didn't change by change of solar zenith angle, and it wasn't affected by optical thickness change, either. It is because 11 ㎛ and 12 ㎛ are infrared channel, so they are not affected by sunlight, and this makes the nighttime observation possible.

The threshold value of BTD was 0.6°K when the satellite zenith angle was 10°, and 1.2°K when the satellite zenith angle was 60°, showing 0.6K difference. When the satellite zenith angle was 10, if optical thickness increased from 0 to 1, BTD value decreased from 1.2K to -1.1K, and when the satellite zenith angle was 60°, it decreased from 0.6K to -3.6K. Therefore, it's found that the larger satellite zenith

angle showed the higher BTD threshold value, and the change according to aerosol thickness was also high. In BT change analysis at 11 ㎛ and 12 ㎛ depending on the zenith angle of satellite, it was found that BT was a little lower at 11 ㎛ channel than that of 12㎛ as the optical thickness increases. As satellite zenith angle increases, optical depth is getting bigger, and more radiation is absorbed at 11 ㎛ channel than 12 ㎛ channel. That is why BT and BTD value showed the difference. In this analysis, while solar zenith angle didn't affect BTD threshold value, the satellite zenith angle made great impact, the latter is the important factor in threshold value calculation and sensitivity.

3) BTD change according to altitude of cloud and Asian dust

As altitude of cloud and Asian dust affect atmospheric radiation transfer, BTD sensitivity depending on altitude was analyzed. BTD showed slight change according to the altitude of Asian dust. When Asian dust was located at altitude of 0~2 km and the optical thickness was 1, BTD value was -1.9K, and BTD value increased as the altitude increased. Asian dust originated from Chinese continent in the size of 0.5~5.0 ㎛ was transferred to North America across the pacific ocean in the altitude of 3.5~4.0 km(Shaw, 1980). The BTD value didn't change much when Asian dust existed between 0~5 km, change of BTD depending on altitude is small as to be neglected compared to other factors.

4) BTD change depending on atmospheric condition

Standard atmospheric condition is determined by temperature and humidity distribution and chemical composition of the atmosphere. Therefore, BTD threshold value change was analyzed by season, latitude and US standard atmosphere and also by various categories in more detail such as tropical region, middle latitude summer, middle latitude winter, high latitude summer, high latitude winter. High latitude winter showed the lowest threshold value of 0.4K and tropical region showed the highest threshold value of 2K. As optical thickness of aerosol increased, difference of BTD depending on standard atmosphere condition decreased. Through this analysis, it was found that the threshold value changed very fluidly depending on the standard atmosphere condition.

Detailed analysis was made to find out what atmospheric factor causes the change of threshold value like this. In the result, the vertical distribution of temperature and humidity in atmosphere affected BTD threshold value much more than other factors. Standard atmosphere distribution was fixed as US standard atmosphere, and the

surface temperature was decreased by 5K from 295 to 275K from surface to top. Water vapor was decreased gradually toward upper layer in the range of 5000~20000 ppmv. When the surface temperature was 295K and 275°K, the threshold value was 0.8K and 0.6K, respectively, which is considered as slight change. The change was also small according to the optical thickness. However, as surface temperature greatly varies day and night depending on earth surface characteristics, threshold value change is considered to be larger. The threshold value changes more sensitively depending on water vapor distribution then temperature distribution. It was found that the threshold value changes largely from 0.5 to 1.8K by water vapor distribution. When BTD showed the value of 0.0~-3.0K with Asian dust, change of threshold value by 1K or more will cause about 30% of error. Therefore, water vapor distribution in the atmosphere should be seriously considered in BTD threshold value estimation.

5) BTD change according to surface emissivity

Surface emissivity was estimated in 11 and 12 ㎛ bands for 14 kinds of surface categories and its impact on BTD was analysed. Surface emissivity data was calculated based on the data from Snyder et al.(1998) and MODIS USCB Emissivity Libarary (http://www.icess.ucsb.edu/modis/EMIS/ html/em.html). BTD threshold value was estimated by earth surface characteristics. BT at 11 ㎛ and 12 ㎛ changed over 2.0° K by surface emissivity. However, as the emissivity at 11 ㎛ and 12 ㎛ changed together by the surface condition, BTD didn't change much and BTD threshold value in general was about 0.4K. But, in the case of arid bare soil, BTD threshold value was the lowest, and when it was compared with other surface type other than snow and ice area, in particular vegetation area, the difference was very low as 0.2~0.3K. When compared with BTD change by Asian dust, it has about 10% of error. BTD threshold value changed a lot in snow and ice area. Therefore, surface type shoud be considered to analyse BTD change.

6) BTD change according to temperature and surface type

Aerosol distribution study based on BTD method shows that BTD values change over time and BTD shows negative value even without aerosol at nighttime. As infrared radiation is emitted proportional to an object temperature, it is closely related to the surface temperature. By the diurnal variation of temperature based on MODIS observation, the temperature greatly changes by at least 30 ° K up to by 70 ° K (not shown). So BTD change tendency is investigated according to the diurnal

suface temperature. In the case of the area with dry soil, which is the origin of Asian dust, BTD changes from -1.6°K to 0.8°K by about 2.4°K according to surface temperature. The big variation like this may include 100% error in BTD values and also this can arise misinterpretation of clean air condition area over aerosol area. In the case of snow/ice area close to ocean emissivity, BTD change from -1.3°K to 1.5°K by about 2.8°K. However, in the case of ocean, the temperature difference on the sea surface at night is as low as about 5°K and BTD value change is about 0.2°K. Therefore, it is considered that BTD value changes more sensitively in continent than on the ocean, and surface temperature and surface characteristics should be seriously considered in BTD-based estimation.

7) BTD change according to surface reflectance

Reflectance of each channel varies according to the surface condition. First, sensitivity was estimated as surface reflectance ranges from 0 to 0.08. When the surface reflectance was 0, BTD value changes from 0.8~-6.1°K, and when it was 0.08, BTD value changed from 0.6~-5.9°K. Even though BTD is not affected largely by surface reflectance, the threshold value had slight change of 0.2°K. At 11㎛ channel, BTD changes from 1∽5°K according to surface reflectance, but BTD value change was small as 12㎛ BT also changes. Therefore, BTD change on surface reflectance can be considered to be neglectable.

3.2. Methodology

Theoretically, BTD method distinguish cloud and aerosol based on 0°K boundary. However, in the result of sensitivity analysis, threshold value greatly changes depending on satellite zenith angle, vertical water vapor distribution in the atmosphere, and temperature and surface type. Depending on the selection of threshold value, strong Asian dust signal may be attenuated, and it can give us false alarm. As pixel-based BTD threshold value changes temporally and spatially, an fixed threshold value can cuase significant error. This problem can be solved only by setting up a background threshold value that varies temporally and spatially.

Aerosol measurement using visible light is done by estimating the background reflection for each pixels on a clear day without aerosol or cloud and then subtracting the value from the measurement on the day of interest (Hauser et al. 2005). The reflectance in clear condition is selected by finding the smallest reflection

at the given pixel from last several days observation. In the similar principle, the maximum BT at 11 μm at the same hour is determined to be defined as clear pixel for last 10 days observation and the BTD at the time is defined as BTV (Background Threshold Value) at the pixel. Asian dust is usually observed in spring when the temperature continues to increase, so when BT at 11μm showed the maximum, it can be regarded to be least affected by cloud or water vapor. Therefore it is defined as clear pixel.

However, in the area frequently affected by cloud and water vapor like ocean area, background threshold value can have highly positive value. It can bring an error in this case, so cloud screening is required. When BTD between 11 μm and 12 μm is bigger than 0.5, it is assumed to be affected by water vapor or cloud and the value is deleted. Therefore, the maximum BT at 11μm is searched in other data, and the BTD maximum at the time is defined as background threshold value.

3.3. Calculation process

Figure 1 shows the hourly BT at $11\mu m$ and $12\mu m$ channels (Fig. 1(a) and (c)) and the difference between 2 BTs(BTD)(Fig. 1(b) and (d)) determined from clear pixel in Seoul and in Yellow Sea using the definition above. On a land area like Seoul, temperature is the highest in the middle of daytime and the lowest just before sun rise. In the ocean, there is almost no change of temperature throughout a day. The pattern of temperature changes over land and ocean is very similar to the ground observation data, so it supports the reliability of the estimated background threshold values (http;//kma.go.kr).

BTD*, the BTD adjusted by subtracting the background threshold value which completed cloud screening from BTD of Asian dust case, was defined as Asian dust index. Figure 2 shows how the Asian dust index was estimated by the suggested algorithm.

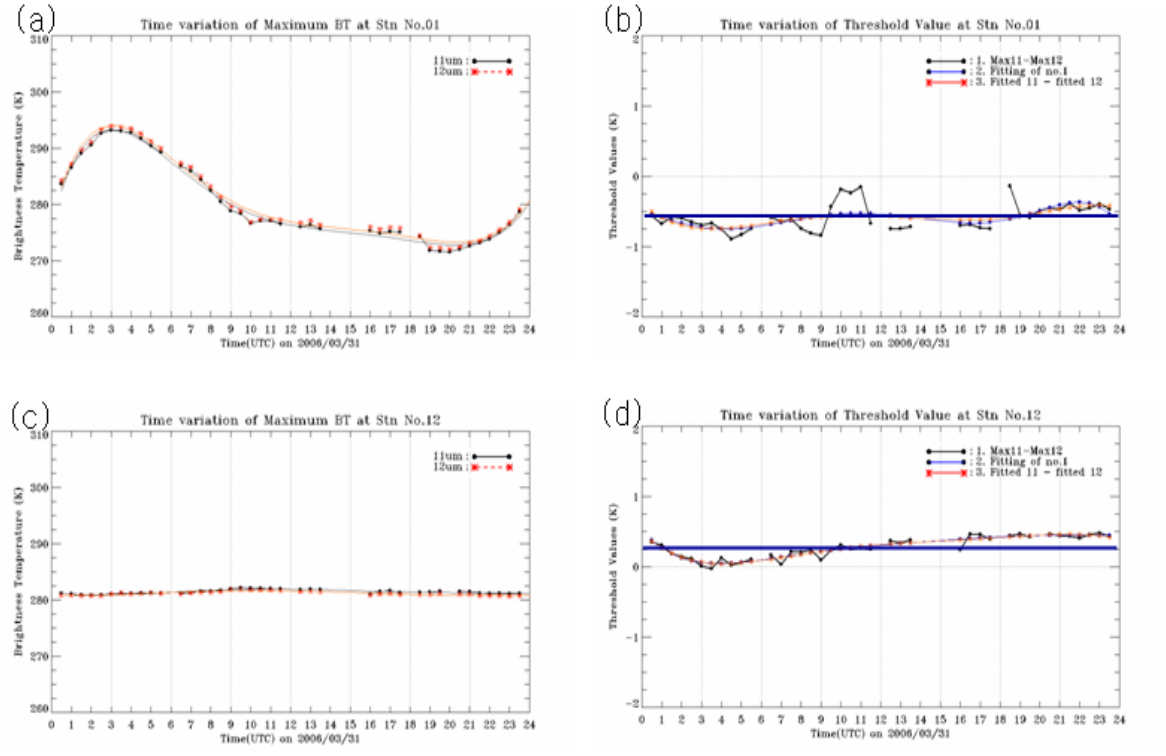

Fig. 1. (a) background brightness temperature of 11μm(filled circle) and 12μm (asterisk) (b) background brightness temperature difference(BTD) between 11 and 12μm for Seoul. (c) and (d) is the same as of (a) and (b), respectively, except for the East Sea at 131°E and 37°N. The line in (b) and (d) is averaged BTD over 24 hours. The time in x-axis is in UTC.

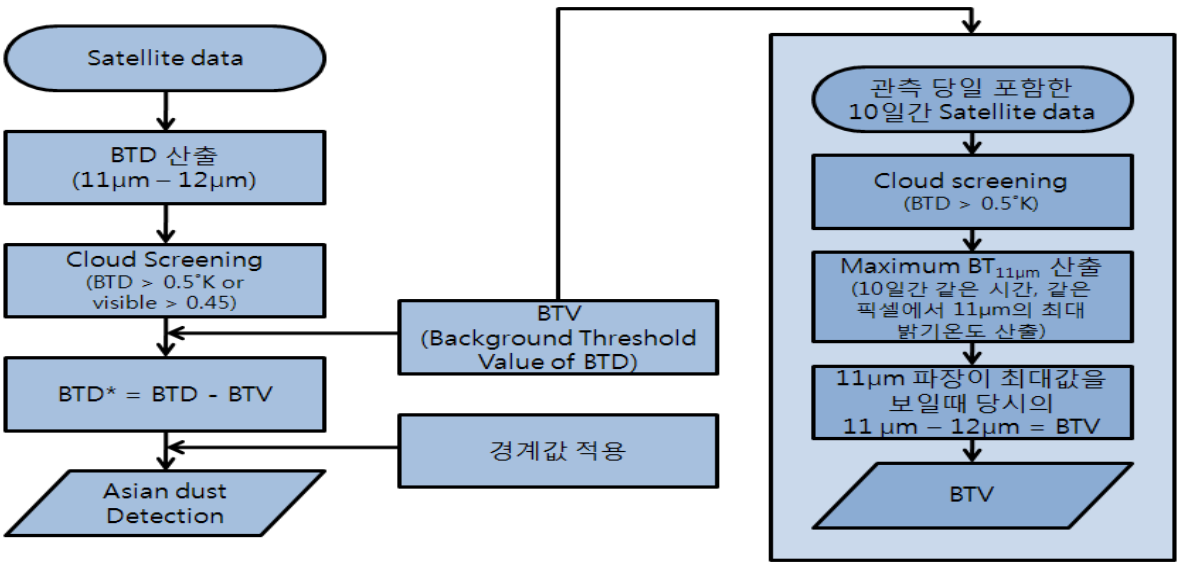

Fig. 2. Flow chart for the Aerosol Index algorithm.

3.4. Evaluation

3.4.1. Evaluation Method

The Asian dust index of BTD* and BTD determined by newly developed algorithm and conventional algorithm were evaluated by the association with OMI AI and score test. Table 1 shows the explanation of the score test used to evaluate.

Table 1. The score test used for the evaluation. Here FAR is False Alarm Ratio and POFD is Probability Of False Detection.

	observed OMI AI			
Forecast Pixel for BTD* and BTD		yes	no	total
	yes	Hits(A)	False Alarm(B)	forecast-yes
	no	Misses(C)	Correct Negatives(D)	forecast-no
	total	observed-yes	observed-no	total(n)

$$Accuracy = \frac{hits + correct\ negatives}{total}$$

$$BIAS = \frac{hits + false\ alarms}{hits + misses} = \frac{\text{for ecast 'yes'}}{observed\ 'yes'}$$

$$FAR = \frac{false\ alarms}{hits + false\ alarms} = \frac{false\ alarms}{\text{for ecast 'yes'}}$$

$$POFD = \frac{false\ alarms}{correct\ ngatives + false\ alarms} = \frac{false\ alarms}{observed\ 'No'}$$

To evaluate the result of algorithm, statistical binary type test scheme was used. This evaluation scheme is to predict one out of two incidents either "Asian dust will occur at each location" or "Asian dust will not occur". For example, a certain threshold value is applied to BTD* and occurrence frequency table is made with yes in case that the result is less than the threshold value and no in case that the result value is bigger than the threshold value. The 2 X 2 frequency table of "yes" and "no" of Asian dust prediction pixel and observation pixel is called as contingency table. OMI AI data were used for determination of yes and no for observation pixels.

This contingency table is useful to find what kind of error occurred. If Asian dust is perfectly detected, there would be only hit and correct, the negative pixels with no pixel in miss and false alarm. Based on this contingency table, indices were calculated by following equation to check the improvement. As Aura satellite is a polar orbit

satellite, it observes Northeastern Asia 2-3 times a day. Therefore, each index was calculated for March 1st 2008, at the time of the satellite passes over Northeastern Asia.

It was defined as Asian dust pixel when OMI AI was over 1.5, and evaluation index was calculated for each range of threshold value of BTD* in 0˚K, -0.1˚K, -0.2˚K, -0.3˚K, and –0.5˚K. The result is shown in Table 3. As a perfect score is 1, it was found that the accuracy was largely improved in BTD* compared to conventional BTD method. As for bias, the perfect score was 1, a value higher than 1 means overestimation and a value lower than 1 means underestimation.

Table 2. The MTSAT observation time lists that matches with OMI observation time (time in UTC)

Times	MTSAT observation time	OMI observation time
	2006/3/26 0433UTC	2006/3/26/ 0429UTC
1	2006/3/27 0333UTC	2006/3/27 0334UTC
2	2006/3/28 0433UTC	2006/3/28 0417UTC
3	2006/3/31 0300UTC	2006/3/31 0310UTC
4	2006/3/31 0500UTC	2006/3/31 0449UTC
5	2006/4/07 0333UTC	2006/4/07 0317UTC
6	2006/4/07 0500UTC	2006/4/07 0500UTC
7	2006/4/08 0400UTC	2006/4/08 0400UTC
8	2006/4/22 0433UTC	2006/4/22 0415UTC
9	2006/4/23 0333UTC	2006/4/23 0319UTC
10	2006/4/23 0500UTC	2006/4/23 0458UTC
11		

Table 3. The results from the score test.

Index / TV	Accuracy		BIAS		FAR		POFD	
	BTD	BTD*	BTD	BTD*	BTD	BTD*	BTD	BTD*
0.0˚K	0.764	0.737	1.740	1.849	0.602	0.640	0.220	0.248
-0.1˚K	0.806	0.864	1.401	0.889	0.541	0.380	0.159	0.070
-0.2˚K	0.839	0.889	1.102	0.677	0.468	0.239	0.108	0.034
-0.3˚K	0.858	0.900	0.893	0.571	0.400	0.146	0.075	0.017
-0.5˚K	0.867	0.895	0.732	0.474	0.342	0.085	0.053	0.008

3.4.2. Evaluation Material

For applying BTD method, the data of MTSAT which has similar function with COMS were used. The Asian dust days observed from the ground and other satellite are selected for this study. To compare the Asian dust index determined in this method, AI observed at OMI for the same period was selected. For AI estimation by OMI observation, Ultraviolet measurements were used. While surface reflectance is relatively low, it responses sensitively to aerosol like Asian dust and fire. That is why ultraviolet is used mostly in comparison of aerosol measurement using satellites.

3.4.3. Method for Time-Space Concurrence

The OMI, the sensor on polar orbiting AURA satellite, is designed to pass the equator around noon because its observation is by the sunlight reflectance. The time it passes the Korean peninsular varies depending on the viewing, but it is usually around 1:00PM. On the other hand, as MTSAT is a geostationary orbit and observation is made at every 30 minutes, the MTSAT observation close to OMI observation time was selected. Spatial resolution of OMI is 23×13 km. and that of MTSAT infrared channel is 4×4 km, the spatial difference was minimized by gridding the both data by 0.25 X 0.25.

3.4.4. Evaluation Result Analysis

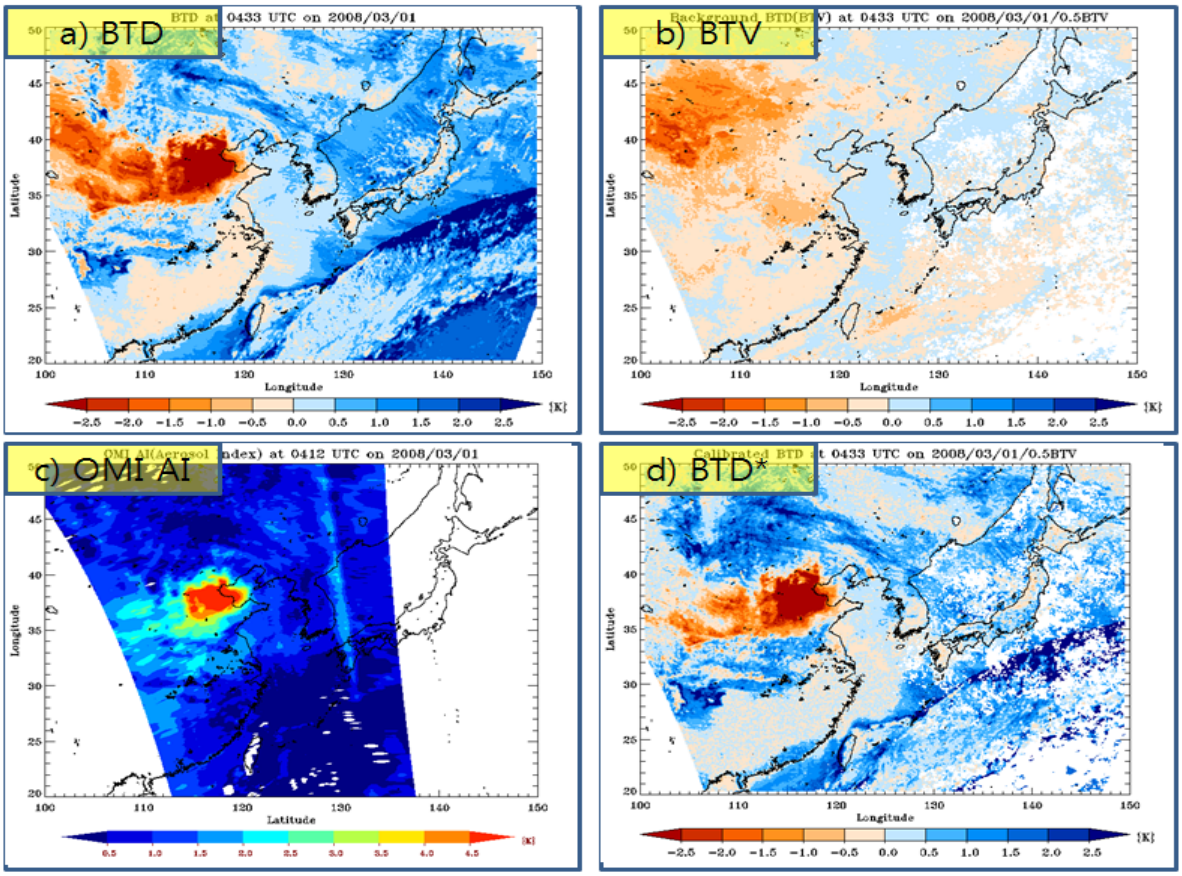

Fig. 3. BTD, BTV, OMI AI and BTD image on March 1, 2008.

Figure 3 shows the Asian dust distribution determined by applying this method to MTSAT observed on March 1, 2008 and Ozone Mapping Instrument(OMI) Aerosol Index(AI). The calculated background threshold value showed different distribution forms depending on day/night, continent/ocean. Continent showed negative value in general. In particular, desert area of Chinese inland showed strong negative value. On the other hand, ocean area showed positive values around 0˚K , manifesting the clear distinction between land and ocean. As the absolute value of negative BTD is higher, Asian dust signal is stronger. The negative difference from threshold value means the decrease of Asian dust signal, and positive difference means the increase of Asian dust signal. Daytime showed more irregular distribution than night and marine area at night showed positive value overall.

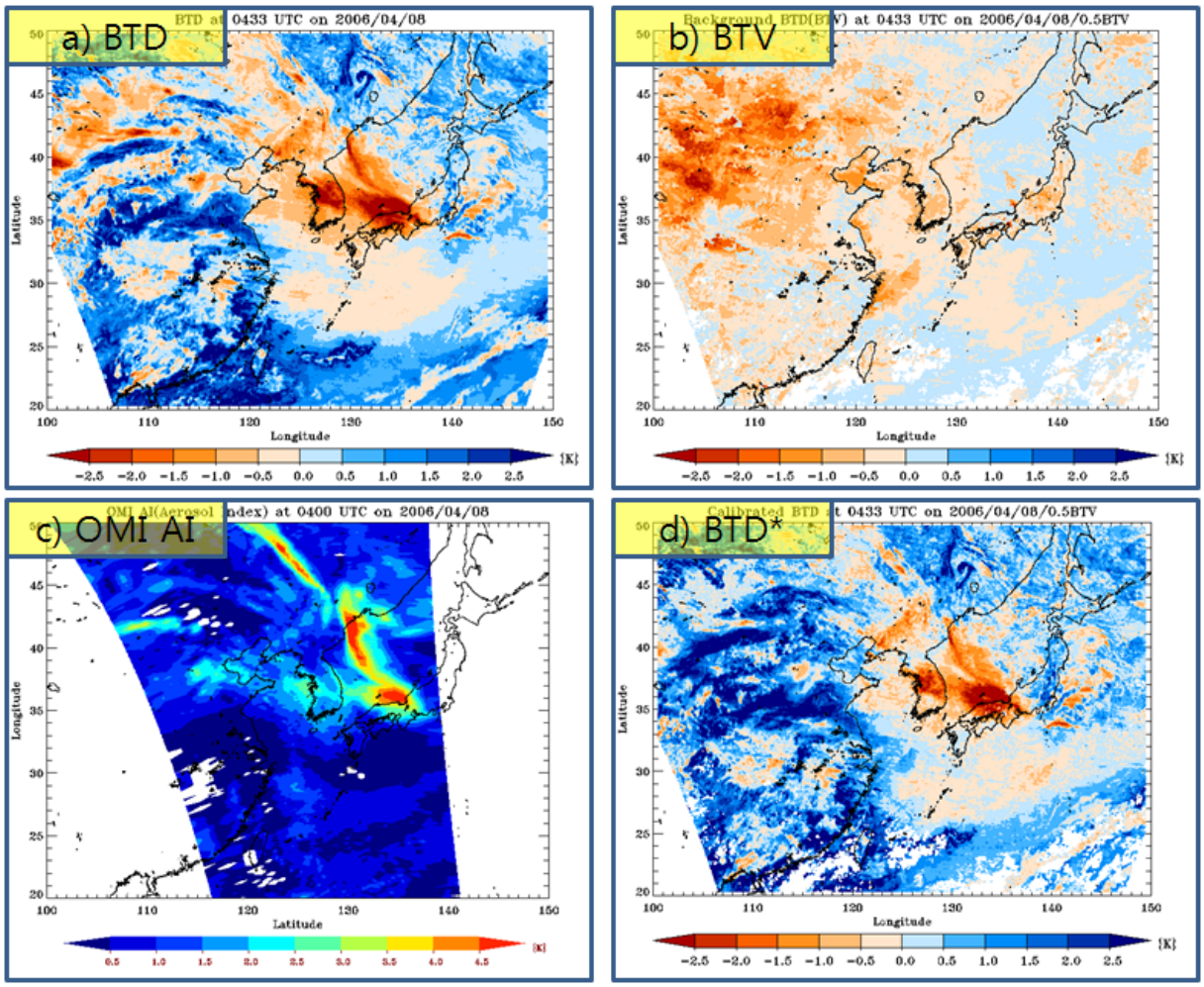

Fig. 4. BTD, BTV, OMI AI and BTD image on April 8, 2006.

Figure 4 shows the Asian dust distribution observed on April 8, 2006. This figure also shows that BTD* is clearly superior to BTD. BTD* reduced error of conventional BTD method significantly. Wrongly detected Asian dust region including desert region in Chinese inland was removed. The weak Asian dust signal detected in the ocean was amplified and the boundary between land and ocean was mitigated. As analyzed in sensitivity result, on a clear day at night, the threshold value of BTD can be shown negative due to cooling down of earth surface, leading false Asian dust signal. Error like this was also much reduced in BTD*.

Figure 5 shows the correlation of Asian dust index and OMI AI determined by BTD* and BTD during the sample dates given in Table 2, varying the background threshold value. Regardless of the change of background threshold value, BTD* developed by this study shows clearly higher correlation coefficient by 0.4 than the one determined by

BTD,

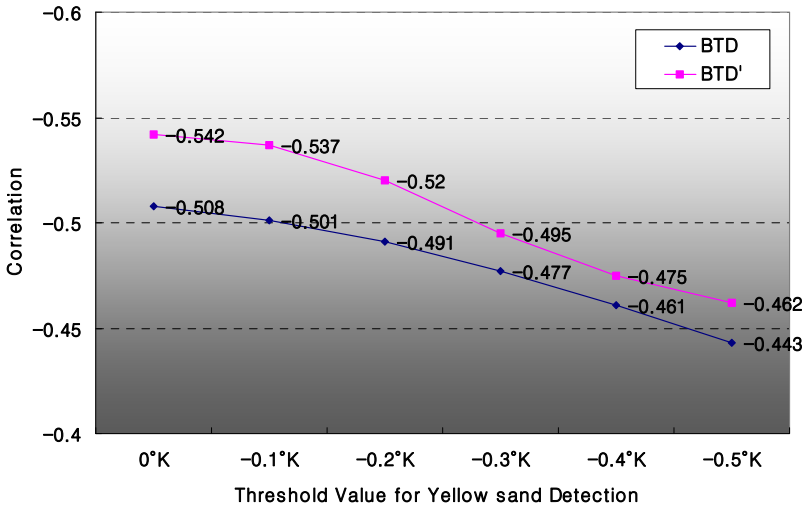

Fig. 5. Regression coefficients for OMI AI and BTD and BTD* with respect to threshold values for the period shown in Table 2.

Statistical test using score test also shows similar result. Figure 3 shows the score test result determined by varying background threshold value. As accuracy and bias get closer to 1, and as FAR and POFD get closer to 0, it means they have close value as OMI AI. In the case of accuracy, BTD* is showing clearly higher value than BTD. In the case of FAR and POFD, BTD* shows clearly lower value than BTD. This is considered to have proven that the Asian dust index determined by applying BTD* is clearly superior than by BTD.

4. Interpretation Method of Result

The method suggested in this study uses the principle that the difference of BT at wavelength bands, 11μm and 12μm, which are windows of atmosphere, is positive for cloud and negative for Asian dust. The absolute value of the negative value becomes higher when there is more Asian dust in the air. However, there are several more factors affecting both wavelength bands, including temperature and condition of earth surface and water vapor present in the atmosphere, which affect the most. This study was done to find out how to adjust the timely and spatially change of the temperature and condition of earth surface. In the method we suggested, background threshold value of

BTD on clear day of the pixel given for 10 days was subtracted from the BTD of the day of observation to make adjustment.

In Figure 3 and 4, negative value refers to the area with high Asian dust signal, and value around 0 refers to clear area. The higher the absolute value of negative value, it is more probable to have Asian dust.

5. Problems and Improvement Possibility

The most important thing in the present algorithm is to deduct background threshold value. Clear pixel was defined to be the day when the highest temperature was observed during 10 days. However, as surface temperature changes according to the condition of the atmosphere and surface type, the day with the highest temperature might not represent the clear pixel on the day of observation. Another problem is that deducted background threshold values by time is not regular and its cause is not known. Satellite observation data from various hours is required for more detail evaluation. However, the evaluation process of aerosol estimation such as Asian dust is constrained since only polar satellite data are available around noon.

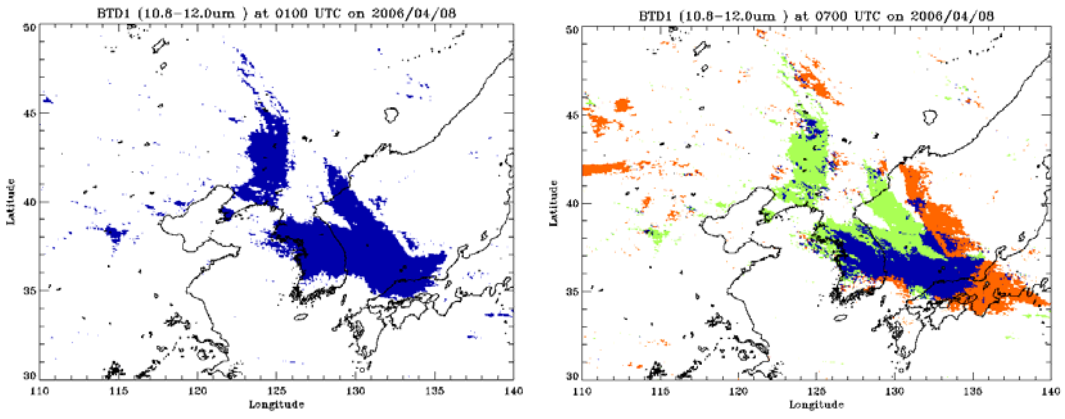

Fig. 6. 11μm~12μm brightness temperature difference at 00 and 05UTC on 8 April, 2006. Green and blue colored areas are at 00UTC, and blue and yellow colored areas are at 05UTC.

To overcome this problem, the advantage of consecutive geostationary orbit observation can be utilized. Figure 6 shows relative change of Asian dust index determined by BTD for 5 hours. As Asian dust moves by upper wind, if hourly change

is compared with wind field, presence of Asian dust in each pixel can be immediately evaluated and then used for supporting weather prediction. The cause of error can be analyzed in detail if wrongly predicted Asian dust pixel data is analyzed based on this. In addition, For BTD* and BTD Asian dust index evaluation, the accuracy can be improved if COMS data are used for evaluation as well as MTSAT.

6. References

Young Wook Lim, Jung Wong, 1989: Study of Heavy Metal Contamination Among Respiratory Dust. Korea Atmosphere Conservation Journal, 5(1), 68 ~ 78.

Ackerman, S. A., 1989: Using the Radiative Temperature Difference at 3.7 and 11μm to Track Dust Outbreaks. *Remote Sens. Environ.* 27, 129-133.

Ackerman, S. A. and K. I. Strabala, 1994: Satellite remote sensing of H_2SO_4 aerosol using the 8 to 12μm window region: Application to Mount Pinatubo, *J. Geophys. Res.*, 99(D9), 18639-18649

Chun, Y., K. O. Boo, J. Kim, S-U. Park, and M. Lee, 2001: Synopsis, transport and physical characteristics of Asian dust in Korea, *J. Geophys. Res.*, 106(D16), 18,461-18,469.

Fukushima, H. and M. Toratani, 1997: Asian dust aerosol: Optical effect on satellite ocean color signal and a scheme of its correction, *J. Geophys. Res.*, 102(D14), 17119-17130.

Gomes, L., and D. A. Gillette, 1993: A comparison of characteristics of aerosol from dust storms in central Asia with soil-derived dust from other regions. Atmos. Environ., 27A, 2539-2544.

Goudie, A. S., 1978: Dust storms and their geomorphological implications, *J. Arid Environments*, 1, 291-310.

Gu, Y., W. I. Rose, and G. J. S. Bluth. 2003: Retrieval of mass and sizes of particles in sandstorms using two MODIS IR bands: A case study of April 7, 2001 sandstorm in China. *Geophys. Res. Lett.* 30(15), doi:10.1029/2003GL017405.

Hauser, A., D. Oesch and S. Wunderle, 2005: NOAA AVHRR derived Aerosol Optical Depth(AOD) over land: A comparison with AERONET data. *J. Geophys. Res.*, Vol.110, D8204, doi:10.1029/2004D005439, 2005

Kaufman, Y. J., D. Tanre, H. R. Gordon, T. Nakajima, J. Lenoble, R. Frouin, H. Grassl, B. M. Herman, M. D. King, and P. N. Teillet, 1997: Passive remote sensing of tropospheric aerosol and atmospheric correction for the aerosol effect, *J.*

Geophys. Res., 102(D14), 16815-16830.

King, M. D., Y. J. Kaufman, D. Tanre, and T. Nakajima, 1999: Remote sensing of Tropospheric Aerosols from Space: Past, Presents, and Future, *Bulletin of the American Meteorological Society*, 80, 2229-2259.

Liu, C. and M. H. Smith, 1995: URBAN AND RURAL AEROSOL PARTICLE OPTICAL PROPERTIES. *Atmos. Environ.*, 29(22), 3293 ~ 3301.

McKendry, I. G., J. P. Hacker, R. Stull, S. Sakiyama, D. Mignacca, and K. Reid. 2001: Long-range transport of Asian dust to the Lower Fraser Valley, British Columbia, Canada, *J. Geophys. Res.*, 106(D16), 18361-18370.

Mishchenko, M.I., I.V. Geogdzhayev, B. Cairns, W.B. Rossow, and A.A. Lacis, 1999: Aerosol retrievals over the ocean using channel 1 and 2 AVHRR data: A sensitivity analysis and preliminary results. Appl. Opt., 38, 7325-7341.

Prata, A. J., 1989: Observations of volcanic ash clouds in the 10-12 window using AVHRR/2 data, *Int. J. Remote Sensing*, 10, 751-761.

Shaw, G. E., 1980: Transport of Asian desert aerosol to the Hawaiian island. *J. Appl. Meteor.*, 19, 1254-1259.

Snyder, W. C., Z. Wan, Y. Zhang, and Y. Z. Feng, 1998, Classification-based emissivity for land surface temperature measurement from space, Int. *J. Remote Sening*, 19, 2753-2774

Sokolik, I. N., and O. B. Toon, 1998: Modeling the radiative characteristics of airborne mineral aerosols at infrared wavelengths, *J. Geophys. Res.*, 103(D8), 8813-8826.

Stow, D., Hope, A., and George, T. 1993: Reflectance characteristics of arctic tundra vegetation from aerial radiometry and videography, *International Journal of Remote Sensing, 14*, 1239-1244.

Toon, I., and J. E. Pollack, 1976: A global average model of atmospheric aerosols for radiative transfer calculations. *J. Appl. Meteor.*, 15, 225-246.

Torres, O., P. K. Bhartia, J. R. Herman, A. Sinyuk, P. Ginoux, and B. Holben, 2002: A Long-Term Record of Aerosol Optical Depth from TOMS Observations and Comparison to AEROENT Measurements, *J. Atmos. Sci.* 59, 398-413.

Wen, S., and W. I. rose, 1994: Retrieval of sizes and total masses of particles in volcanic clouds using AVHRR bands 4 and 5, *J. Geophy. Res.,* 99(D3), 5421-5431.

Whitby, K. T., 1978: The physical characteristics of sulfur aerosols. *Atmos. Env.*, 12, 135-159.

Yu, T., and W. I. Rose, 2002: Atmospheric correction for satellite-based volcanic ash mapping and retrievals using "split window" IR data from GOES and AVHRR.

J. Geophy. Res., 107(D16), 10.1029/2001JD000706.